QUENCH PROTECTION

K.H. Mess
DESY, Hamburg, Germany

Abstract
Quench protection starts with the design of the magnets. Hence tools to estimate the stability of a magnet against temperature perturbations are discussed. Stable magnets quench reluctantly, of course. The low expansion rate may in turn have an influence on the hot-spot temperature. Methods to measure and estimate quench expansion are presented and the problems with quench detection and energy extraction are discussed using existing solutions as examples.

1. TRANSITION TO THE NORMAL CONDUCTING STATE

A strand of a superconducting cable consists of matrix material, for example, copper or aluminium, which surrounds the hard (type II) superconductor, for example, NbTi. Let the strand have the perimeter P and the cross sectional area A, and let it be completely immersed in liquid helium at the bath temperature T_B to keep it superconducting. An external magnetic field B is applied perpendicular to the wire. The wire will remain in the superconducting state if the current density in the superconductor $J = I/(1\text{-}f)A$, the external field B, and the temperature T are all below the "critical surface", where f is the matrix fraction of the wire. Figure 1 shows this "surface" that describes the phase transition. The critical surface of a piece of superconductor depends on the chemical consistency and the treatment during production. Approximate properties of NbTi-copper composite conductors, useful for calculations, can be found in the literature [1], [2], [3]. Superconductivity vanishes for any set of two parameters, if the third parameter increases beyond the critical value. Some authors [3] distinguish between transitions by simultaneous current and field increase (along arrow C, conductor limited quenches) and by local temperature fluctuations (along arrow E, energy deposited quenches). The distinction helps to identify the reason for quenches and to find possible cures. Moreover, the current density is normally constant throughout the coil or large fractions of it, while the temperature and the field may vary. In a magnet the field B correlates with the current I. Thus magnets operate on a load line, as the line C in Fig. (1) indicates for $T = T_B = 4.2\text{K}$.

If the superconducting compound wire has for some reasons a local temperature above the bath temperature, as indicated in Fig. 2, the thermal energy varies along the strand because of the heat flow. If the temperature is high enough Joule heat generation will take place. Wire motions in the magnetic field, cracking epoxy, eddy current heating and other distributed sources may add further heat. The heat conduction through the surface of the strand to the coolant will cool the wire. All energy variations will result in a local change of the thermal energy. The equation for the heat balance in a piece of conductor of length dx can be written:

$$C_{avg}(T)\frac{\partial T}{\partial t} = \frac{\partial}{\partial x}\left(k_{avg}(T)\frac{\partial T}{\partial x}\right) + Q(T) + g_{dist}(t,x) - W(T)\,. \qquad (1)$$

Heat conduction, Joule heating, additional distributed heat sources, and the energy absorbed by the coolant determine the change in temperature. C_{avg} is the volumetric specific heat capacity, averaged over the wire. The thermal conductivity depends on the direction of heat flow. In the axial direction the heat conductivities add up according to their relative area like $k_{avg}(T) = fk_m(T) + (1-f)k_s(T)$, where the subscripts m and s stand for matrix and

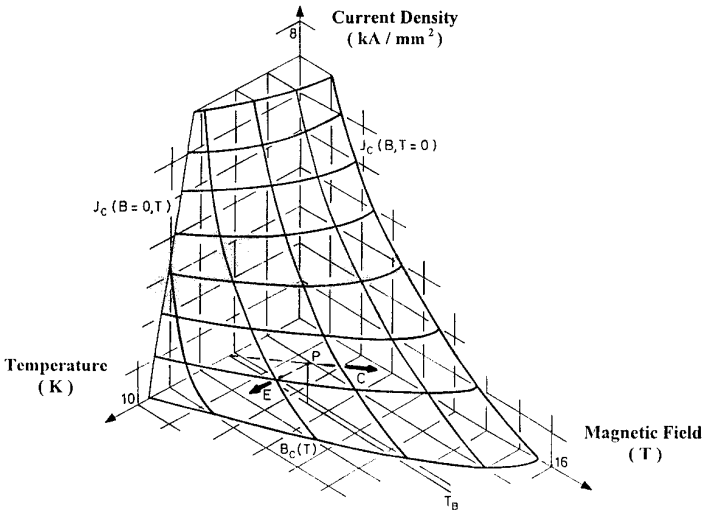

Fig. 1 The phase transition surface of NbTi

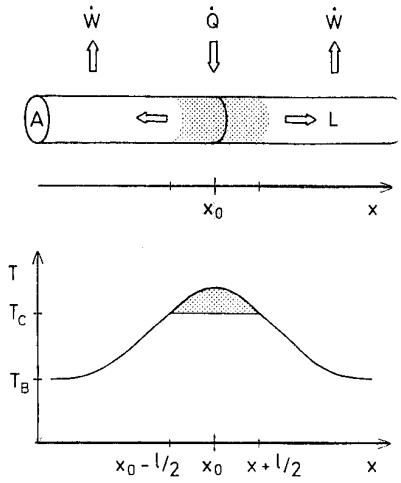

Fig. 2 Sketch of the heat balance in a quenching cable and of a possible temperature profile

superconductor respectively. In the radial direction the expression for the heat conductivity must take the distribution of filaments in the matrix and a possible cladding with solder or varnish into account, which renders the transverse heat conductivity ill defined. It is customary to hide the general lack of knowledge by simply scaling the transverse heat conductivity from the axial heat conductivity by applying some factor. Copper and aluminium are by far the better conductors and also transport the heat much better than NbTi. It is therefore a fair approximation to ignore the contribution to the heat conductivity by the superconductor altogether if material with a small resistivity ρ_m at low temperatures is selected as matrix.

The cooling term in Eq. (1) depends on the temperature difference times the heat transfer coefficient *h*, which varies with temperature and cooling conditions.

The Joule heating term needs detailed explanation. If the temperature is low enough the current density in the matrix $J_m = I_m / f \cdot A$ will be zero and the current will entirely flow in the superconductor with a density $J = I / ((1-f) \cdot A)$. For convenience the average current density is called $J_{avg} = I / A$.

Close to the critical surface some of the flux in the superconductor starts moving. The changing total flux through the superconductor induces an electrical field, which shows up as if there were a resistance. The resistances of the flux-flow and of the matrix act in parallel. The increase in matrix current will be such that the voltage due to the surplus current beyond the critical current in the superconductor, which feels the flux flow resistivity ρ_f, equals the voltage in the matrix:

$$V_m = J_m \rho_m = (J_s - J_c)\rho_f = (J - J_m - J_c)\rho_f \ . \qquad (2)$$

As the flux flow resistance is quite large for small surplus currents approximately all current above the critical current is transferred to the matrix. The so called current-sharing model states that the superconductor carries as much current as possible up to the critical current density J_c. Any additional current flows through the matrix.

As the critical current density depends almost linearly on the temperature for a given field, the current-sharing (or heat generation) temperature is:

$$T_g = T_B + \left(T_c(B) - T_B\right)\left(1 - \frac{J}{J_c(B, T_B)}\right). \tag{3}$$

Below the current-sharing temperature the Joule heating is zero because the superconductor carries the current. Above the critical temperature the superconductor is practically free of current and the average resistivity is $\rho_{avg} = \rho_m / f$ because the resistance of NbTi exceeds the resistance of good copper by a factor 2000.

Figure 3 illustrates the current-sharing. The thick line indicates the current density in the superconductor; the dotted line shows the current density in the matrix.

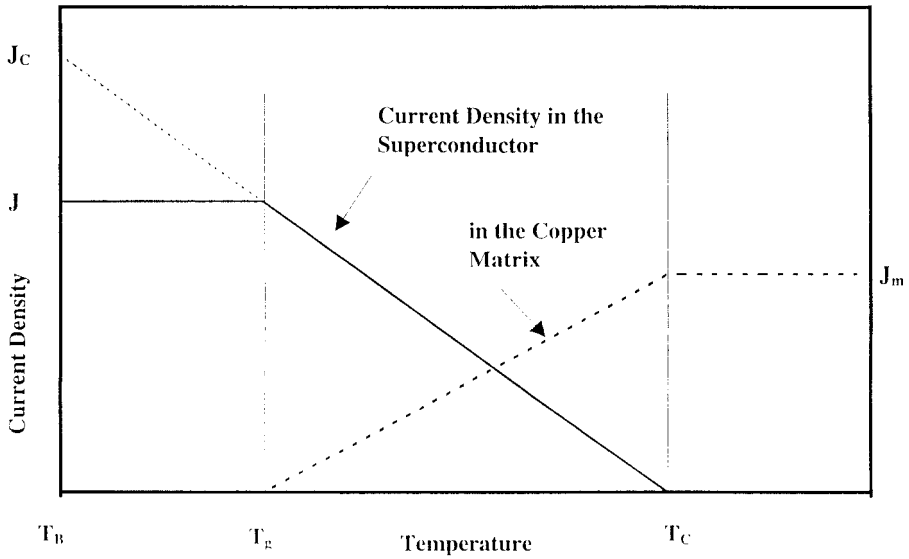

Fig. 3 Distribution of the current density between superconductor and matrix in the current sharing region

The Joule heating equals the total transport current density times the electrical field:

$$Q(T) = J_{avg} \cdot E = J_{avg} \frac{dU}{dx} = \frac{I}{A}\frac{dU}{dx}. \tag{4}$$

The differential voltage dU depends on the temperature difference over a distance dx along the wire and equals the current through the matrix times the differential resistance dR_m. Using the linear approximations for the matrix current density one calculates the Joule heating term as:

$$Q(T) = \begin{cases} 0 & \Leftarrow T \le T_g \\ \dfrac{\rho_m(T) J_{avg}^2}{f} \dfrac{T - T_g}{T_c - T_g} & \Leftarrow T_g \le T \le T_c \\ \dfrac{\rho_m(T) J_{avg}^2}{f} & \Leftarrow T \ge T_c \end{cases} \tag{5}$$

Usually knowledge about the distributed heat sources g_{dist} is quite limited. All magnets have welds or solder joints somewhere in the cable. A good solder joint has a resistance of $10^{-9}\,\Omega$. Hence a typical current of 5000 A creates a steady heat load of 5 μW. This can already present a stability problem under some circumstances.

Accelerator magnets, fusion reactor magnets or detector magnets for high energy experiments will always be exposed to some level of radiation. A bunch consisting of 10^{11} protons of 1 TeV deposits an enormous energy density of 10 J/cm^3 in a typical copper-stabilised NbTi coil.

Other heat sources are related to the Lorentz forces in the magnet. They deform the coil. This may result in movements or bending of conductors and hence in friction [4]. For magnets under SSC design conditions [3] a 10 μm movement over a conductor length of 500 μm is sufficient to release 10 μJ.

2. STABILITY

Quench protection means first of all protection against quenches. This is best achieved by constructing a magnet that hardly quenches under normal operating conditions. What can reasonably be expected and which are the sensitive parameters?

Little can be done against occasional temperature disturbances in the conductor. The cooling and the heat capacity of the cable determine the stability against such disturbances. Its extension in space and time and the shape of the temperature distribution will determine whether the zone of disturbance grows or decreases. The minimal zone that cannot be cooled away is often called the “minimum propagating zone” or MPZ [5].

Equation (1) describes the heat balance along the conductor. The most interesting questions are: What are the conditions that cause the expansion of a normal zone, and what is the expansion rate? What are the conditions for a normal zone that does not expand? If a current-sharing or normal conducting zone is very short, the heat can be conducted away. Alternatively if the heat produced is small enough, it can be cooled away on the helium wetted surface. Thus there are two extreme cases. In the first case heat sources can be assumed to be uniformly distributed along the wire. That is equivalent to the absence of longitudinal heat conduction. All cooling takes place locally through the surface to the helium. In the second case, a very short hot spot expands by heat conduction along the wire in both directions. The heat flow into the helium is neglected because the surface is small or well insulated.

2.1 Cooling of an isothermal wire

If a long region is normal conducting or current-sharing, the heat conduction along the wire is insignificant and the helium absorbs all heat Q locally. Under these conditions the critical current density is reached at $T = T_B$. In steady state the power generation must be less or equal to the cooling. The ratio of Joule heating to surface cooling is called the Steckly parameter α_{St}.

$$\alpha_{st} = \frac{\rho_m J_C^2 (1-f)^2 A}{f P h (T_C - T_B)} \tag{6}$$

If the cooling always dominates over heat generation (for $\alpha_{St} < 1$) the wire is cryogenic stable. A coil with $\alpha_{St} < 1$ can not quench provided liquid helium is available. Large coils like solenoids in the experiments at storage rings or for tomography, or in toroids to store magnetic energy are in this very favourable situation. But accelerator or fusion reactor magnets are usually far away from this ideal state. In the HERA dipoles, for instance, $\alpha_{St} = 22.3$; so the coils are definitely not cryo stable. Full cryogenic stabilisation is uneconomical for accelerator magnets. One has therefore to accept that such magnets may and will quench.

In reality, the normal zone does not extend to infinity nor can the cooling through the surface be ignored. Taking both heat-conduction and cooling into account simultaneously one arrives at the Maddock [6] criterion, also called "equal area theorem". It states that heat generation and heat removal should cancel each other globally but not necessarily locally. The conductor will be stable, provided the surplus heat at the hot spot can be conducted to a cooler place, where surplus of cooling is available. The difference of the integrals over cooling and heating along the wire from the superconducting region up to the hottest spot is what counts. If the difference vanishes, the conductor stays stable. As the temperature increases monotonously, the integration over space can be replaced by integration over temperature. The theorem states:

$$\int_{T_B}^{T_H} \left[\frac{Ph}{A}(T - T_B) - \frac{A}{P} Q(T) \right] k(T) dT = 0, \tag{7}$$

where T_H is the maximum temperature of the normal zone.

2.2 Cooling by heat conduction along the wire

To find the smallest normal conducting region that does not propagate, and to estimate the energy needed to create such a minimum propagating zone let us rewrite Eq. (1) in three dimensions and study the expansion of a small normal conducting zone. The aim is a solution for the stationary case without external cooling (adiabatic limit). Additional cooling would allow a larger zone to be stable. It is therefore possible to ignore the cooling, if one is only interested in the minimal zone.

The thermal conductivity in the longitudinal direction, κ_x, is well known, while the radial heat conduction must be estimated. It turns out to be sensible to set $\alpha^2 = k_r / k_x$. α is typically 2-3%. Equation (1) can be rewritten in spherical co-ordinates introducing a scaled radial co-ordinate $R = r/\alpha$.

$$\frac{d^2 T}{dR^2} + \frac{2}{R}\frac{dT}{dR} + \frac{(1-\varepsilon) Q}{k_x} = 0. \tag{8}$$

The factor $(1-\varepsilon)$ takes care of the fact that a fraction $\varepsilon \approx 0.1$ of the coil (if Rutherford cable is assumed) consists of voids filled with helium.

The solution of Eq. (8) consists of three parts. Close to the origin, in the region with Joule heating, (that is, inside a "sphere" of radius R_g) the temperature is:

$$T = T_g + A\frac{R_g}{R \cdot \pi}\sin\left(\frac{\pi \cdot R}{R_g}\right), \tag{9}$$

with
$$R_g = \sqrt{\frac{k_x\left(T_C - T_g\right)}{(1-\varepsilon)Q\left(T_g\right)}}\cdot\pi = \frac{\sqrt{f}}{J_{avg}}\sqrt{\frac{k_m\left(T_C - T_g\right)}{(1-\varepsilon)\cdot\rho_m}}\cdot\pi\,. \tag{10}$$

If the temperature exceeds the critical temperature Eq. (8) overestimates the heat production. Thus the Eqs. (9) and (10) describe an upper limit only. In real space the minimum propagating zone is an ellipsoid, oriented along the quenching wire, with a total length of $2\cdot R_g$ and a transverse diameter of $2\cdot R_g\sqrt{\frac{k_r}{k_x}} = 2\alpha R_C$.

Outside the heat producing zone, $\left(R \geq R_g\right)$, the heat generating term in Eq. (8) vanishes and the solution is

$$T_{out} = T_g(1-(1-\frac{R_g}{R})A)\,.$$

At the cold side the temperature reaches the bath temperature in principle at infinity. In reality the zone cannot extend that far. Firstly it would take a very long time to reach a steady state and secondly an infinite energy would be required. Far away, at a distance $R_{cold} = x\cdot R_g$, the longitudinal heat flow is insignificant compared to the cooling by the helium through the insulation. At this point and beyond, Eq. (8) is invalid. The longitudinal temperature gradient does not need to be continuous any more. The cold boundary determines the constant *A* and hence the maximum temperature inside the minimum propagating zone. If the temperature reaches the temperature of the bath at $R_{cold} = x\cdot R_g$, the temperature profile can be written as

$$T = \begin{cases} T_g + \dfrac{x\left(T_g - T_B\right)R_g}{(x-1)\pi R}\sin\left(\dfrac{\pi R}{R_g}\right) & \Leftarrow R \leq R_g \\ T_g - \dfrac{\left(R - R_g\right)x\left(T_g - T_B\right)}{R(x-1)} & \Leftarrow x\cdot R_g \geq R \geq R_g \\ T_B & \Leftarrow R \geq x\cdot R_g \end{cases} \tag{11}$$

Figure 4 shows as an example four temperature profiles for minimum propagating zones in the DD0019 prototype magnet for SSC [3] at its nominal operating point (at that time). The bath temperature is 4.35K in this case and the field about 6.9T. The four curves correspond to x = 1.25, 1.5, 1.75 and 2 respectively. The heavily drawn curve describes the most probable profile (x = 1.5), as explained below. The horizontal scale gives the longitudinal size of the disturbance.

The energy needed to create a minimum propagating zone depends on the actual temperature profile and hence on the boundary where the bath temperature is reached again. Because the temperature depends only on the radius the energy is described by the double integral

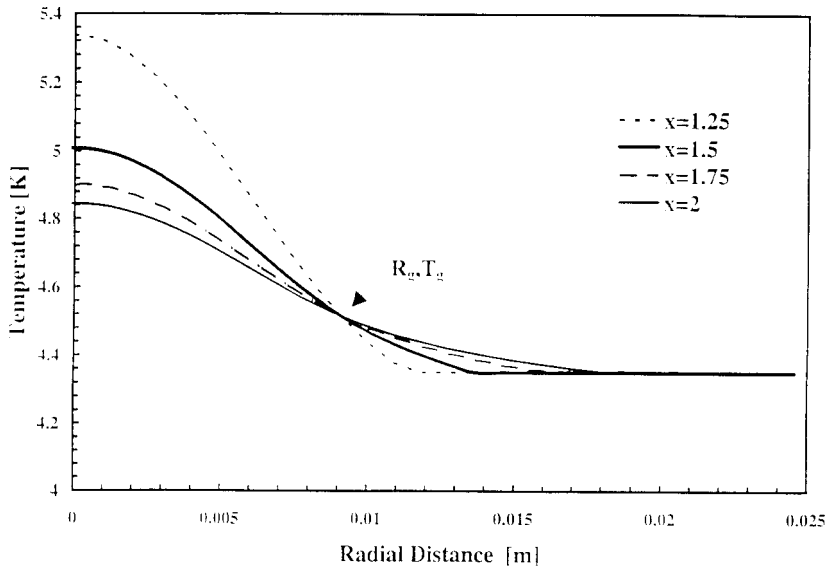

Fig. 4 Temperature profiles of minimum propagating zones. The bath temperature is reached at the radial distance $r = xR_g$.

$$E = \int_0^{xR_g} \int_{T_B}^{T(r)} C_{avg}(\vartheta) d\vartheta \; 4\pi (r\alpha)^2 dr . \qquad (12)$$

The factor α^2 takes into account that the lateral dimensions have to be rescaled to physical dimensions. Analytic calculations of this integral are quite complicated. Even approximations lead to integrals that have to be solved numerically. It turns out that (12) has a shallow minimum between $1.4 < x < 2.5$. The energy needed to create the temperature distribution varies here by less than 20% as a function of x; the exact minimum depends on other parameters, however. The quoted minimum energy to produce a minimum propagating zone is a good measure of the relative stability of cable configurations or operating points.

Figure 5 shows the minimum propagating energy for a typical HERA dipole magnet (at 4.5 K) and for the SSC prototype magnet DD0019 (at 4.35 K) as a function of the magnetic field, assuming α = 3%. The bath temperatures correspond to their nominal values respectively. The arrows indicate the peak fields in the coils under nominal conditions. Obviously the SSC magnet reaches a much higher field. At the nominal operating point the minimum propagating energy has dropped below 10 μJ, in fortuitous agreement with measurements [3] and other calculations [7]. The HERA design is considerably more conservative. The minimum propagating energy at nominal conditions is 0.15 mJ and the corresponding volume is $7.1 \cdot 10^{-9}$ m^3.

It is often assumed that a lower bath temperature would provide for a more stable operation. Figure 6 shows the minimum propagating energy for the HERA coil as a function of the bath temperature. The gain in safety is quite moderate when lowering the bath temperature because the heat capacity is so small. However, below the lambda point the improved heat removal changes the situation completely.

The size of the minimum propagating zone depends on the geometric mean of heat conductivity and the electrical conductivity properly scaled by the relative fraction of copper.

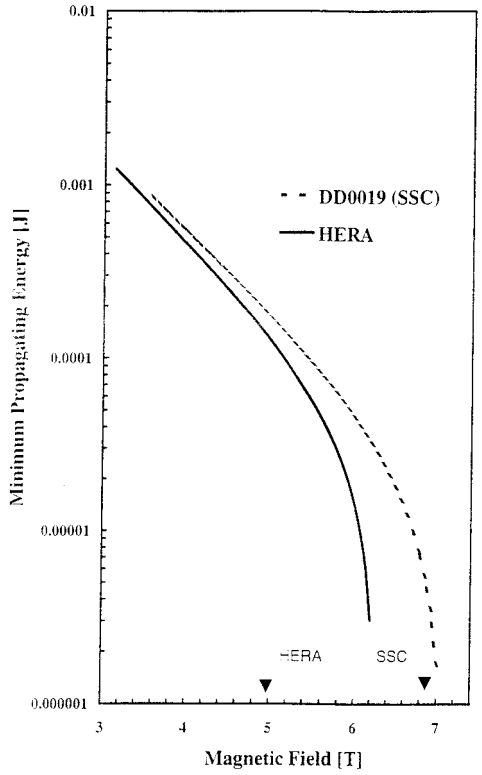

Fig. 5 Minimum propagating energy as a function of the magnetic field for a typical HERA dipole (T_B = 4.5 K) and the early SSC prototype magnet DD0019 (T_B = 4.35 K). The arrows indicate the respective peak field values under nominal operating conditions.

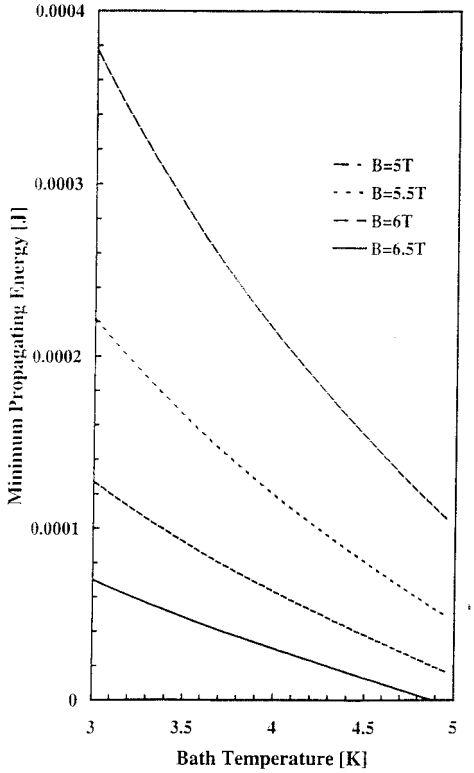

Fig. 6 Minimum propagating energy for a typical HERA dipole as a function of the bath temperature for four values of the highest magnetic field in the coil.

Removal of matrix material decreases the size of the minimum propagating zone if the amount of superconductor is unchanged. It also decreases the minimum propagating energy, because less material needs to be heated above the current-sharing temperature.

3. QUENCH EXPANSION

One would like the largest possible minimum propagating zone for magnet protection, because a large zone also means a "large" energy to trigger the quench. One may hope that such a kind of disturbance is rare and hence the likelihood of quenches is small. However once a quench has started, one would like the normal conducting zone to expand quickly. Often the magnet has to absorb the stored magnetic energy or at least a sizeable fraction of it. A large conducting volume results in a low energy density and hence a low maximum temperature.

Once a normal zone has started to grow it will continue to do so as long as the current density and the magnetic field are high enough. The low heat conduction of the insulation and latent heat of the helium content in the cable impede the transverse expansion. Therefore the normal zone will expand dominantly along the cable.

Quench velocities in a piece of cable in the field of an extra magnet are easy to measure. Voltage taps distributed along the wire are sufficient to detect the arrival of the normal zone by measuring the resistive voltage over the normal zone. Figure 7 shows a typical example. The voltage rises linearly when the normal zone expands between two voltage taps.

Thereafter the voltage rises slowly because the resistance is almost constant below some 25 K.

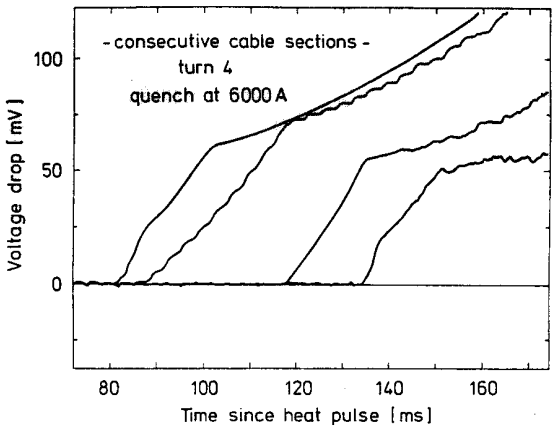

Fig. 7 Measurement of the voltage drop over consecutive cable sections during a quench as a function of time

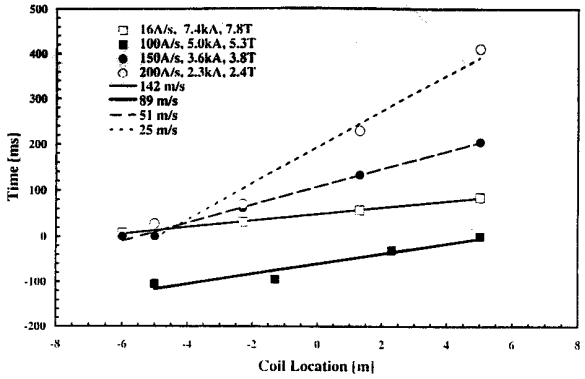

Fig. 8 Measurements of the time of detection of a local field distortion in "quench antenna" coils as a function of the coil position. The four sets of data correspond to quenches occurring at different ramp rates and hence currents and magnetic fields in the SSC dipole prototype DCA 312. The lines are fits to the data [14].

Measurements at real magnets are more difficult. Basically four methods exist to measure the quench velocity in a magnet. One can try to attach voltage taps to the coil during assembly. This does not work too well because the attached wires are always a hindrance during the coil compression under curing. At best a few connections in the magnet heads, where access is somewhat easier, are possible.

Another method was used to observe quenches in a short HERA prototype magnet [8]. Devices that carried needles like a porcupine were inserted into the coil aperture. The needles could be expanded and pierced into the inner coil layer by turning a key from one of the magnet ends. Several porcupines could be inserted. However, it is both difficult and dangerous to insert such a device because insufficient alignment results in shorts between the coil windings.

A developing quench is rather violent and produces ultrasonic noise. It was observed that the flux redistribution indeed makes noise [9] which can be picked up by microphones. In particular, if the magnetic field changes rapidly, this method of monitoring has some advantages because the acoustic emissions are not electromagnetic and thus immune against electromagnetic noise. Acoustic measurements with several microphones can also reveal the origin and propagation of a quench. The drawback is, however, that quite often acoustic signals are emitted that do not correspond to a quench or vice versa [10].

The most elegant way to observe, measure, and trace back quenches has recently been invented by Krzywinski [11] and since been used at CERN [12] and SSCL [13], [14].

A moving wire or the current redistribution between strands at the front of an expanding normal zone creates field distortions. They induce signals in pick-up coils, properly located inside the free aperture of the quenching magnet. Such antennae can be made insensitive to changes of the main dipole field by quadrupolar or sextupolar coil arrangements. This works

very much in the same way as in the measurement of the magnetic multipole components. The twin aperture magnets for LHC offer the favourable possibility to subtract signals of corresponding radial coils in the two apertures. Radial coils are easier to produce to the same dimensions and the results are easier to interpret.

To detect quenches and observe the quench propagation it is sufficient to insert four radial coils, rotated by $\pi/2$, preferentially all mounted on the same shaft and covering the length of the magnet under investigation. To cancel dipole contributions either a corresponding coil in the second aperture or the properly weighted average of the other three coils can be used. Alternatively, sets of coils can be made that measure quadrupolar and sextupolar field components, both regular and "skew", i.e., shifted by $\pi/4$ and $\pi/6$ respectively. For quadrupole magnets, of course, sextupolar and octupolar pick-ups are necessary.

The starting point (radius and azimuth), the direction and the change of the magnetic strength characterise the transverse motion of a magnetic moment. Four different coils are sufficient to measure this. At SSCL this technique allowed to locate the quench origin at the inner edge of a particular winding turn.

The longitudinal position of the quench origin can be deduced from the development of the signal with time. To achieve this at least two, preferentially many, sets of pick-up coils are stacked along the length of the magnet. Depending on the circumstances, many identical sets of coils can be mounted on a common shaft or the sets are positioned individually, employing the technique of the moles, as for harmonic measurements. If more than one set of coils detects the quench and if the quench velocity is reasonably constant the axial position of the quench origin can be determined to better than 1 cm.

To measure the velocity of the quench front two methods can be used. In the simplest case one uses the pick-up coils as voltage tap replacements. The distance between the pick-up coils is known and times of the arrival of the quench front can be detected. Figure 8 shows an example from SSCL [14]. The aim of the experiment was to find the reason for the ramp rate dependence of the apparent critical current. Hence the various ramp rates given in the index correspond in reality to different current densities and fields as indicated. Note that the measured velocities are as large as 100 ms^{-1}.

In the second approach, the magnetic flux in the pick-up coil is calculated, by integrating the induced voltage. In Fig. 9 this is done for four consecutive pick-up coils in a one-meter long LHC model magnet [12]. The time intervals at which the propagating normal zone passes by can easily be measured and compared to the slope. Again about 100 ms^{-1} are observed. One may even argue that the velocity increases slightly. In Fig. 10 [12] the signals in three pick-up coils at the same longitudinal position are shown for a somewhat longer time. The second bump (or dip, respectively) corresponds to the current redistribution in one of the adjacent turns. The quench obviously needs 14 ms to propagate azimuthally by one turn. Unfortunately, a complete and consistent set of quench velocity measurements in a large magnet has not so far been published.

The quench antenna method is also useful to study other phenomena. It has been observed that sharp signals are accompanied by mechanical oscillations. The damping of the oscillations depends on the absence or presence of the flux iron. Obviously the potential of the method has not yet been fully exploited.

Measurements on cables showed that the normal zone expands at a constant velocity, except in the very beginning, where the manner in which the quench has been initiated has some influence. In real magnets, however, the magnetic energy has to be dumped and the current has to be decreased in order to protect the coil from melting. The rapidly changing

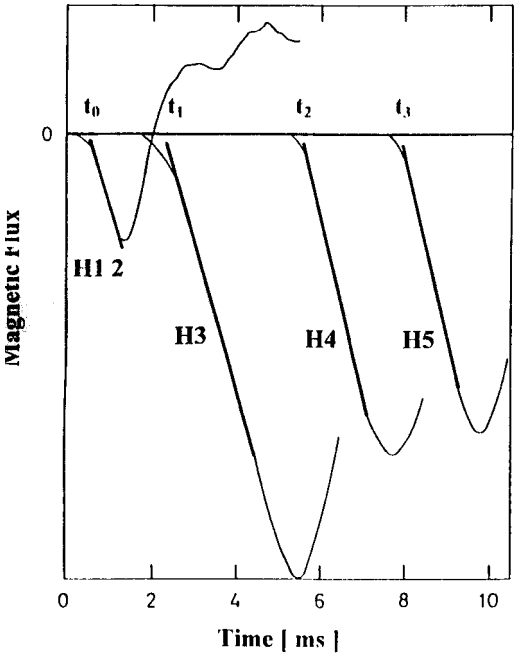

Fig. 9 The development of magnetic flux in a series of "quench antenna" coils as a function of time shows the longitudinal propagation of the quench in a LHC model magnet [12].

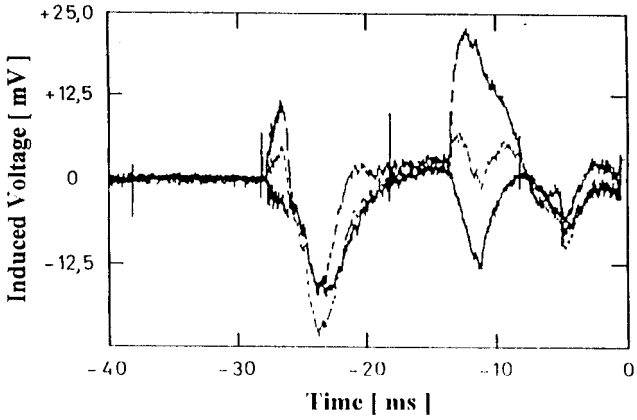

Fig. 10 The superimposed voltages of three "quench antenna" coils of the same longitudinal section show signals when the quench front of one cable passes by and when, after 14 ms, the normal zone has expanded to the adjacent winding.

magnetic field causes movements of the coil and eddy current heating. (This may even happen at normal ramp rates, as was demonstrated by the measurements of Fig. 8.) The helium may be blasted along the wire, preheating the wire ahead of the front. All these effects are difficult to take into account. Needless to say, approximate explicit formulas can only be calculated under the assumption that all material parameters depend on temperature in very simple ways. Often some averaged values have to be assumed.

In the calculations for the quench velocity the cable is imagined as a homogenous piece of metal with direction dependent heat conductivity. The longitudinal heat conductivity is high. The radial conductivity is low and not well known. The superconducting material, the "dirty" copper in the centres of the strands, the poor contact between the strands, and finally the helium in the voids contribute to the lateral conductivity in a complicated manner. Nonetheless, one can schematically write the radial quench velocity inside the cable as

$$v_r = \sqrt{\frac{k_r}{k_x}} v_x . \tag{13}$$

It is tempting to apply the same technique as used in deriving the minimum propagating zone and the temperature profile. This leads however to integrals that do not have a closed form representation. One has therefore to start the analysis at a time at which the quench is already well in progress. At such a late time the radial expansion has come to a temporary halt at the surface of the wire or cable, because the heat conductivity in the helium-filled insulation is very low and the latent heat comparably large. The quench propagation happens mainly along the wire. Therefore a surface-cooled rod resembles the quenching cable, neglecting all transverse expansion for the moment. In such a picture the radial temperature

gradient vanishes everywhere but on the cooled surface. Thus heat conduction is longitudinal only and the one-dimensional description is quite adequate.

In the simplest approximation one can ignore the current sharing, all temperature dependencies and the cooling. The result is the velocity in the adiabatic limit. It applies for well insulated and relatively heavily-stabilised cable only. However, it gives the order of magnitude for current densities close to the critical density, provided later mentioned complications can be ignored.

In the adiabatic limit, with constant heat capacity and constant heat conduction, and without current-sharing, the quench velocity can be calculated to [2]:

$$v_{ad} = \frac{J_{avg}}{C_{avg}} \sqrt{\frac{\rho_{avg} * k_{avg}}{(T_S - T_B)}} \ , \tag{14}$$

where J_{avg} and ρ_{avg} are averaged over the conductor and T_S is the temperature at which all Joule heating is assumed to take place in the absence of current sharing. Using the Wiedemann-Franz-Lorentz law, which relates electrical and thermal conductivity, Eq. (14) can be written as $\left(L_0 = 2.45 \cdot 10^{-8} \mathrm{W\Omega K^{-2}}\right)$

$$v_{ad} = \frac{J_{avg}}{C_{avg}} \sqrt{\frac{L_0 T_S}{T_S - T_B}} . \tag{15}$$

Heat capacity and resistivity are not constants and current-sharing and cooling can usually not be ignored. In particular cooling can decrease the normal zone again. That would formally correspond to a negative velocity, which Eq. (14) cannot describe. Various approximations have been tried. However, theoretical formulae are mainly useful for interpolating measurements because it is only on the basis of a measurement that one can decide which approximations may be adequate.

M. Wilson [2] takes both steady-state contributions and transient terms into account. Using the relative current density ($i = J / J_C$) the steady-state contribution is formulated in terms of the ratio of cooling on the surface and the heating:

$$y = \frac{hP(T_S - T_B)}{AJ_{avg}^2 \rho_{avg}} = \frac{(T_S - T_B)}{(T_C - T_B)\alpha_{St} i^2} . \tag{16}$$

The transient term *z* compares the latent heat with the heat capacity:

$$z = \frac{Q_L}{C_{acg}(T_S - T_B)} . \tag{17}$$

Combining all effects Wilson finds for the quench velocity:

$$v = v_{ad} \frac{(1-2y)}{\sqrt{yz^2 + z - y + 1}} . \tag{18}$$

Without transient effects, Eq. (18) can be rewritten in terms of the relative current density *i* and the Steckly parameter α_{St}

$$v = v_{ad}\,\frac{1-2y}{\sqrt{1-y}} = \sqrt{\frac{hkP}{AC^2}}\,\frac{\dfrac{(T_C - T_B)}{(T_S - T_B)}\alpha_{St} i^2 - 2}{\sqrt{\dfrac{(T_C - T_B)}{(T_S - T_B)}\alpha_{St} i^2 - 1}}. \qquad (19)$$

With the special assumption $T_S = (T_g + T_C)/2$ Eq. (19) becomes

$$v = \sqrt{\frac{hkP}{AC^2}}\,\frac{\alpha_{St}\, i^2 - 2 + i}{\sqrt{1 - i/2}\,\sqrt{\alpha_{St}\, i^2 - 1 + i/2}}. \qquad (20)$$

Cherry and Gittelman [15] assumed that all Joule heating appears suddenly at $T_S = T_C$, which simplifies the formula (19) to

$$v = \sqrt{\frac{hkP}{AC^2}}\,\frac{\alpha_{St} i^2 - 2}{\sqrt{\alpha_{St} i^2 - 1}}. \qquad (21)$$

More elaborate formulae can be found in the literature that modify Eq. (20) slightly to fit data somewhat better. None of them describes the high quench velocities in long SSC and LHC dipoles mentioned earlier.

Many factors and mechanisms contribute to the expansion of the normal zone in a magnet but are omitted in the calculations. Incidentally, large and rapid changes of the magnetic field and the current result in a further velocity increase [16], as do thermo-hydraulic effects.

Thus, the quench performance of a new design can at best be roughly estimated and modelled. Measurements on a sizeable piece of cable under realistic conditions are strongly advisable to gain insight into which quench expansion mechanism dominates. The quoted formulae may then be used to interpolate between measurements.

4. HEATING OF THE COIL AFTER A QUENCH

4.1 Hot-spot temperature

The quenching region is at all temperatures ranging from the bath temperature up to a maximum temperature which is found at the point where the quench was initiated. The hottest spot is also the spot most in danger and hence one has to be concerned mostly with this peak temperature. As a simplification local adiabaticity is assumed, because it is always a conservative assumption. Furthermore a quench lasts only about one second which is an order of magnitude less than large scale heat exchange in a cryostat. Under this assumption the locally produced heat results in a local temperature rise:

$$J_{avg}^2(t)\rho_{avg}(T)dt = C_{avg}(T)dT\,. \qquad (22)$$

All quantities are averaged over the winding cross section, including insulation and helium in the voids. Equation (22) reads after rearrangement and integration:

$$\int_0^{\infty} J_{avg}^2(t)dt = \int_{T_B}^{T_H} \frac{C_{avg}(T)}{\rho_{avg}(T)} dT = J_0^2 \tau = F(T_H) \tag{23}$$

The rearrangement implies that $\rho(T)$ does not depend explicitly on the time. This is not exactly true. Hence an effective resistivity should be used as approximation.

For a given coil the function $F(T_H)$ can be used to estimate the maximum temperature T_H. $F(T_H)$ depends only on known material constants and can be calculated. The integral over the squared current density is easily determined in the case of a single magnet. In fact, for simplicity only the integral over the square of the current is often calculated and quoted in units of $10^6 A^2S$, called MIITS. Here the current density squared is used in order to be applicable to all similarly built cables.

A direct measurement of the temperature is cumbersome and requires many temperature sensors in the coil. Alternatively, one can determine the average temperature between two voltage-taps from the resistance, i.e., from the voltage drop. Figure 11 shows such a set of measurements [8] plotted against the integral over the squared current density. To relate that to currents, one has to know that the cable area was $1.32 \cdot 10^{-5}$ m^{-2}. The fully drawn curve shows $T_H(F)$, which is the inverse of the function $F(T_H)$ calculated for a HERA type coil. The equivalent curve for a pure copper coil $(\rho_{4.2K} = 10^{-10}\,\Omega\text{m})$ is drawn dashed. The case of pure NbTi cannot be illustrated in the same figure. The curve would essentially coincide with the vertical axis because the large resistivity results in a dramatic heating. Despite the fact, that both $C$and ρ are complicated functions of the temperature, the function $T_H(F)$ can usually be approximated fairly well as a parabola with some offset.

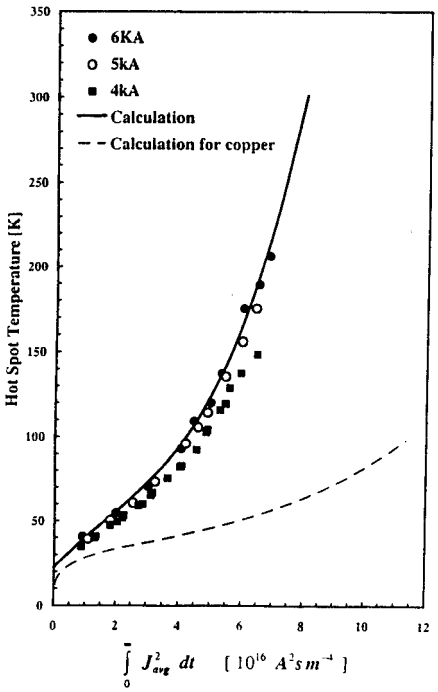

Fig. 11 Hot-spot temperature in a short test dipole for HERA as a function of $\int J^2 dt$: full curve calculated, dashed curve for pure copper $(\rho_{4.2K} = 10^{-10}\,\Omega\text{m})$.

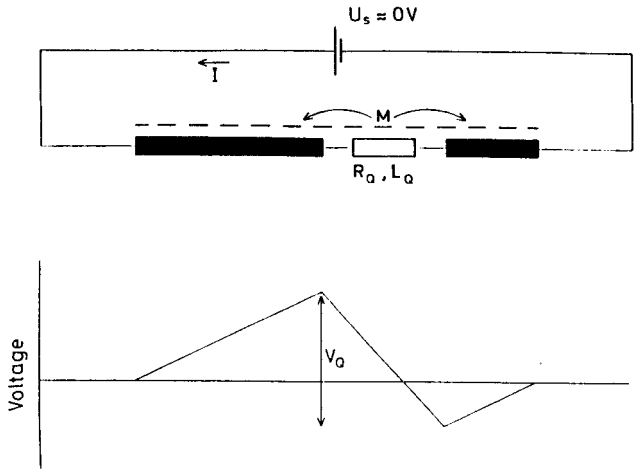

Fig. 12 Equivalent electrical circuit of a quenching magnet and the voltage distribution

The hot spot temperature increases roughly as the square of the current density. This is so because the characteristic time for a quench is roughly inversely proportional to the quench velocity. This in turn is roughly proportional to the current density. In heavily stabilised cable, as is used in the interconnection region between two magnets, the copper properties dominate completely. In these regions a quench can last until the adiabaticity fails after some tens of seconds. The coil, however, reaches at the hot spot a temperature of 100 K in 0.3 seconds.

Good engineering practice would call for 100 K as the upper limit, because the thermal expansion and the mechanical stresses in the coil and support structure start to increase above this temperature. Common practice is however, to go far beyond this point in order to save coil volume, conductor, and hence cost.

One could believe that a current decay time of less than a second may cause high voltages across the terminals of the quenching magnet. Referring to Fig. 12 the voltage can be written as $V_Q = I\ R_Q - \left(L_Q + M\ \right)\frac{dI}{dt}$ and $L\frac{dI}{dt} = I\ R_Q$, because the power supply is assumed to be an ideal current source. L is the inductance of the coil, M the mutual inductance between the normal conducting and the superconducting parts of the magnet. R_Q denotes the resistance and L_Q the inductance of the normal conducting part. Combining the two equations yields

$$V_Q = I\,R_Q\left(1-\frac{L_Q+M}{L}\right)\approx I\,R_Q\left(1-\frac{M}{L}\right) \tag{24}$$

which is always less than or equal to $V_Q^{\max} = I\ R_Q$.

4.2 Numerical calculations

Equation (1) cannot be integrated analytically even if all material properties are assumed to be constant, although most of them depend in reality on the temperature and on the magnetic field. Also approximate solutions fail if external actions, like firing of heaters or bypass thyristors (diodes) to control the hot spot temperature, are to be taken into account. A series of numerical programs has been written to simulate quenches on the computer. The first program published was "QUENCH" [17]. Starting with a current I_0 at the time t_0 the quench velocity is calculated using the calculated magnetic field and the corresponding critical temperature to determine the material properties. Assuming a constant expansion speed the volume at the time t_1 is calculated. Now the average temperature in the normal conducting volume V_1 and the current decay, if applicable, is determined. In the next step the material properties are recalculated using the new temperature, a new normal conducting layer is added, and the temperatures in the inner layers are updated. Each layer keeps its own record of temperature history. Magnetic field and temperature distribution determine the total coil resistance and hence the resistive voltage drop at any time interval. From the external protection resistors or diodes, the inductance, and the coil resistance the coil current can be calculated which is then used for the next time interval. At this point also inductive couplings and other complications can be taken into account. For the transverse expansion either of the two approximations, mentioned above, can be used. The simple Euler algorithm with variable material constants converges acceptably provided the time steps are small enough. In a similar fashion K. Koepke predicted successfully the behaviour of the TEVATRON magnets [18]. These programs as well as the adopted version of QUENCH for HERA [19] or QUENCH-M [20] are bulky FORTRAN programs specially tuned for a particular magnet type and protection circuit. The ideas lead Pissanetzky and Latypor [21] to a modern version, applicable to magnets with a single or with multiple coils, with or without iron, operating in

the persistent mode or from external power. The method assumes again that a quench starts at an arbitrary point of the coil and propagates in three dimensions. Multiple independent fronts can coexist. Local magnetic fields and inductive couplings of the coils are calculated by the finite element method. All properties, like fields and temperatures, are obtained by solving the corresponding equations at each point in space and time. For the LHC magnets Hagedorn and Rodriguez-Mateos designed a different generally applicable simulation package. The general simulation tool, called QUABER [22], is based on a professional tool, called SABER (trademark of Analogy Inc.). Bottura and Zienkiewicz [23,24] developed a finite element program for magnets with "cable-in-conduit", that are magnets with forced helium flow. All programs mentioned above and many variants of them are able to describe the "typical" quench fairly well. However the result of the model calculation depends essentially on the assumptions. It is advisable to investigate as many different input assumptions as reasonable to determine the uncertainty in the calculations.

5. QUENCH DETECTION AND EXTERNAL SAFETY CIRCUITS

The minimum response necessary to prevent conductor burnout when a quench occurs is the disconnection of the power supply. This requires of course the detection of the quench. Several signals can be used to sense a quench. Acoustic emissions precede a quench and follow it. This signal, however, is not very specific because noise emission is not always accompanied by a quench. A resistive voltage $U_q = R_q I$ builds up when a normal zone grows and expands. The rising resistance leads also to a change in current which in turn induces an inductive voltage. In the same fashion an inductive voltage arises when the current changes for other reasons or whenever the coil is magnetically coupled to a coil with changing current [25]. Somehow the inductive voltages have to be cancelled. In the simple case of a single coil, as indicated in Fig. 13a, a single bridge circuit will be a reliable solution. For this purpose a centre tap on the magnet coil is needed and the bridge has to be balanced to better than 0.5%. Once set properly, which may be tedious, the bridges can stay unchanged for years as experience shows. Of course, this method can never detect a quench that develops in both half coils identically. Some additional measures exclude this rather exotic case. In a large system, for example, the bridge method can be repeated for groups of magnets.

Instead of subtracting the inductive voltage by a bridge directly, one can also measure it by some additional device and subtract it from the coil voltage electronically. Figure 13b indicates as an example the measurement with an additional field coil. Alternatively the average voltage of a large set of identical magnets in series can serve as a measurement of the inductive voltage. In either case, problems may arise with the dynamic range, the initial adjustment and eventual drifts with temperature.

Magnetically coupled coils, like stacked correction coils or the windings in fusion reactor magnets, present a particular problem. Current changes in any of the coupled coils induce voltages in all other coils too. Hence the subtraction method has to be expanded to all combinations of all coils. This procedure is somewhat akin to the Gaussian elimination in matrix diagonalisation [25].

The magnet coils float during a quench at an unpredictable potential with respect to ground. The measurement technique has to take care not to destroy the magnets by more than one unintended short to ground. Thus it is advisable to add a resistor in series with the potential tap as close to the coil as practicable in order to limit the possible current to ground and hence the damage. If one applies the bridge detection method high-valued series resistors will decrease the sensitivity. In this case a protection with high voltage fuses is possible. In fact the simplest high voltage fuse for this purpose is a piece of wire-wrap wire, as used in electronics, at a sufficient distance from conducting material. Note that the fuses have to be tested continuously as parts of the quench detection circuit.

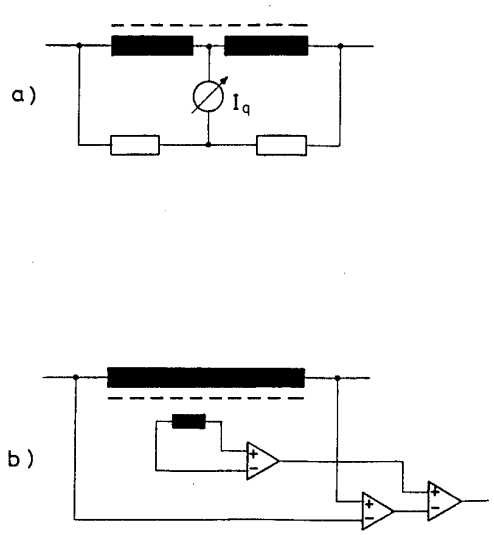

Fig. 13 Quench detection by a) measuring the current through a bridge or b) comparing the total voltage with the inductive voltage.

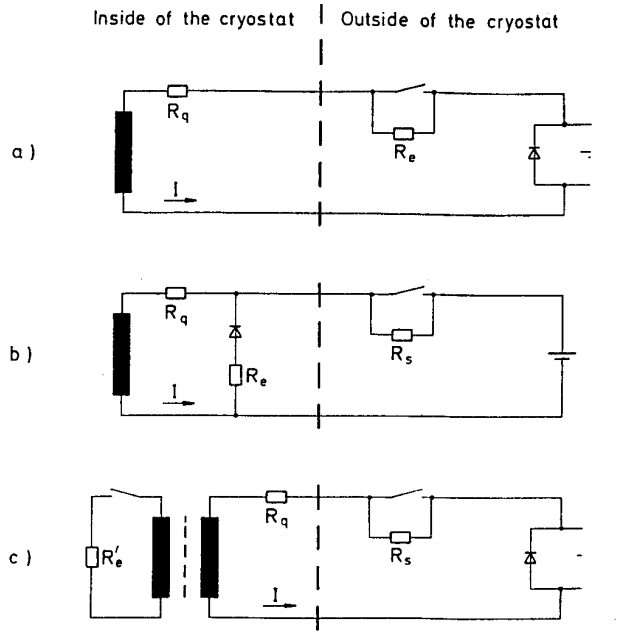

Fig. 14 Possible energy extraction schemes for a single magnet: a) external resistor, b) internal diode and resistor plus external resistor, c) magnetically-coupled resistor.

After the detection of the quench the stored magnetic energy has somehow to be dumped. Rephrasing the power supply to pump the energy back into the mains is possible but usually too slow. Basically all ideas about how to "protect" superconducting coils have been well known for many years [26]. For a single magnet, one can switch off the power supply and dissipate a large fraction of the stored energy by one of the circuits sketched in Figs. 14a, b and c. In circuit (a) the current continues to flow through a diode ("free wheel diode") and a load resistor R that determines basically the maximum voltage $U_{\max} = I_0 R$, the exponential decay time $\tau = L/R$, and hence the hot spot temperature. In circuit (b) an extra diode has been added. It could also be installed inside the cryostat as a so called "cold diode". The current will commute partially into the diode branch once the diode knee voltage is reached. This is a few tens of a volt at room temperature and a few volts at 4.2 K. The current will commute independent of the position of the current switch and the quench detection. In the worst case the diode will melt, but not the magnet. Circuit (c) contains an inductively-coupled resistor R'. This can be the support cylinder of a large solenoid or some other structural element. The heat produced in R', because of the change in the primary current and the magnetic coupling, can be used to accelerate the quench propagation. This solution, termed "back quench", is preferred for slowly ramped magnets but it is not directly applicable for fast ramping superconducting devices.

To summarise, a number of reliable methods have been developed to protect a single magnet after a quench. The quench signal has to be detected and discriminated from noise signals. The power supply has to be switched off without interrupting the magnet current. The stored energy has to be dissipated in suitable devices. If necessary, the quench can be spread artificially by activating heaters in or at the windings.

6. PROTECTION OF A STRING OF MAGNETS

An accelerator consists of large number of magnets in series. A fusion reactor magnet, even worse, consists of a large number of magnetically-coupled coils. The protection of such a string or group of coils is a challenge. For example, the inductance in the HERA ring adds up to L = 26.5H. At 5.5 T, 470 MJ are stored in the ring; an energy sufficient to melt 780 kg of copper.

Unfortunately, a simple switch, as in the case of one magnet, cannot work. A magnet is barely able to absorb its own stored energy. Simple switching-off dumps almost all stored energy into the quenching magnet and destroys it. On the other hand, energy extraction with external resistors would require an enormous resistance and hence a voltage of more than 300 kV.

The recipe is therefore:

- detect the quench,
- isolate the quenching magnet,
- spread the energy,
- subdivide the inductance (if possible).

The principle is best discussed by explaining a few examples. Figure 15a shows the quench detection system of the TEVATRON, the first large superconducting accelerator. It is based on the measurement of voltage differences. Average voltage differences are calculated, including the inductive voltages during ramps, and compared with the measured values. A significant discrepancy indicates a quench. The large values for the resistors, chosen for safety reasons, together with the cable capacity introduce a sizeable signal distortion that has to be corrected.

The system developed for HERA (Fig. 15b) is based on bridge circuits for each magnet. Additional bridges over a number of magnets increase the redundancy. A radiation-resistant magnetic isolation amplifier that is insensitive to noise pickup amplifies the bridge current. A similar but more versatile version has been proposed for UNK [27]. For the LHC also a bridge circuit is in discussion. However, isolation amplifiers with semiconductors are presently favoured.

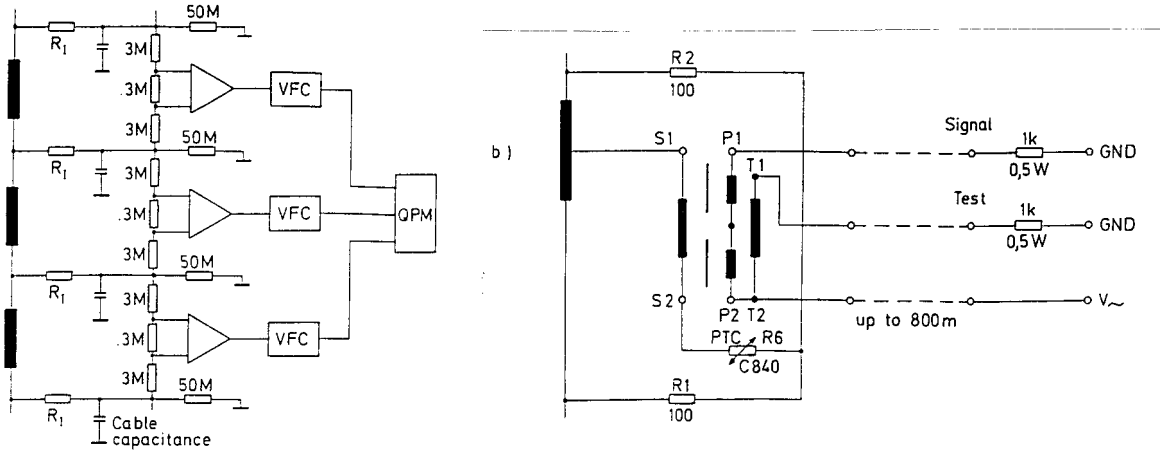

Fig. 15 Quench detection circuits used in large systems, a) TEVATRON, b) HERA

Next the energy of the unquenched magnets has to be kept away from the quenching magnet. Basically, guiding the main current around the magnet achieves this effect. Figure 16 shows an equivalent circuit diagram. The total inductance L of the magnet string is much larger than the inductance L_1 of a single magnet. Hence the main current I decays with a much larger time constant than the current I_Q in the quenching magnet. The differential equation for I_Q is (neglecting diode voltage drops)

$$L_1 \frac{dI_Q}{dt} + I_Q R_Q(t) = \left(I - I_Q\right) R_b \,. \tag{25}$$

Since $R_Q(t)$ grows with time an analytic solution is not available. But once the whole coil has become normal one arrives at a steady state solution

$$I_Q = I \frac{R_b}{R_b + R_Q} \approx I \frac{R_b}{R_Q}. \tag{26}$$

To minimise the current remaining in the coil, the resistor R_b in the bypass line should be made as small as possible.

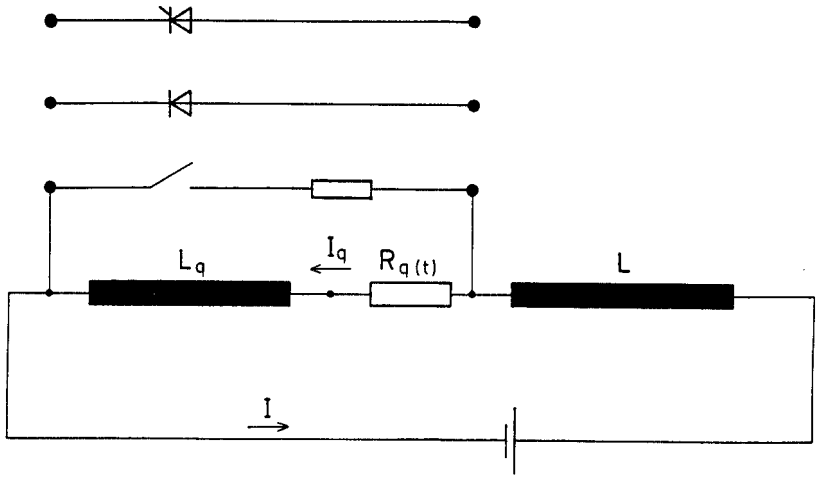

Fig. 16 Equivalent circuit of the bypass of a quenching magnet

Two basic solutions exist. Thyristors act as fast switches at fast ramping machines like the FNAL TEVATRON, SSC or UNK. Figure 17 shows part of the electrical circuit for the TEVATRON. In the TEVATRON magnets the return bus is integral part of the coil and has to be protected. Therefore half the magnets are fed by one bus with half a winding powered by the return bus. The interleaving other half of the magnets is connected in the opposite way. Also shown are the heaters that are needed to distribute the stored energy in a magnet group evenly. The energy of the rest of the ring is bypassed by thyristors. They have to be mounted outside the cryostat and therefore current feed-throughs are needed. These require a very careful design since their electrical resistance (which is the main contribution to R_b) should be small. Their thermal resistance, on the other hand, should be large to avoid a heat load on the liquid helium system. During a quench the safety current leads heat up considerably which brings the connection points to the superconductor in danger of quenching also. In addition a fast recooling time is also an important design criterion. The development of high temperature superconductor current feed-throughs may alter the situation considerably.

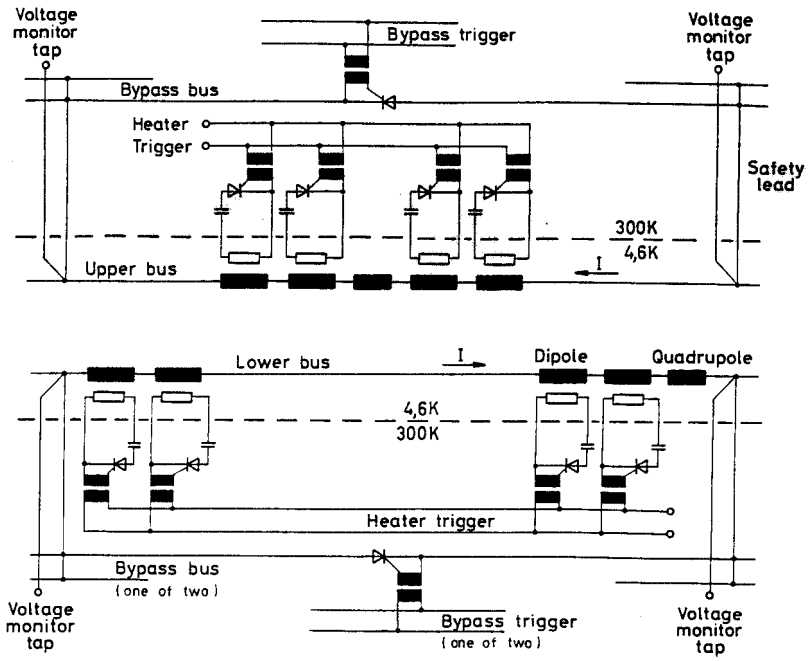

Fig. 17 The magnet connections in the TEVATRON. Dipoles and quadrupoles share two busses. Groups of magnets are protected against the total stored energy by bypass thyristors.

Diodes can replace the thyristors in storage rings that have a low ramp rate and hence small inductive voltages during the normal operation. Cottingham [28] first proposed for ISABELLE to mount diodes inside the liquid helium cryostat. This solution has several advantages. The bypass resistance is normally much smaller. Each magnet can have its own bypass diode. There is no heat load on the cryogenic system due to the safety leads. Finally, the cryostats are easier to build and cheaper if the current feed-throughs are missing. This concept has since successfully been adopted or is proposed for HERA, RHIC and LHC.

The bypass diode has to be selected carefully. Firstly, the diode should have a low dynamic resistance and this should not change as a result of aging or neutron bombardment. Secondly, the proper backward voltage has to be selected carefully. High voltage diodes have a thick p-n junction that is susceptible to radiation damage and which has a large resistance. On the other hand, if magnets in a string quench, not all will quench simultaneously. The inductive voltage that develops during the ramp down will concentrate on the still superconducting magnets and may exceed the backward voltage of the diode. Note that the backward voltage depends on the operating temperature. The extraordinary high current in the LHC magnets and the expected level of radiation pose severe constraints on the cold diodes. Nevertheless promising solutions have been found [29].

Relatively conservative magnets, as the HERA and RHIC magnets, do not in principle need artificially quench spreading, in particular if every magnet has its own bypass. Quench heaters need some energy storage, some firing electronics, and feed-throughs into the cryostat. The heater band has to be in close thermal contact with the coil, because the heat must reach the coil as fast as possible. In fact, the best place is in-between the two coil layers [30]. This is of course hazardous. Good heat conduction means little electrical insulation and hence the risk of shorts to the coil. In summary, quench heaters are costly and a potential danger themselves. However, for safety against quenches in the coil heads, even the HERA dipole magnets are equipped with heater strips, very much as in the TEVATRON magnets. For the LHC magnets to avoid excessive energy densities artificial quench spreading is essential.

Finally, it is necessary to subdivide the machine into as many independent current circuits as feasible. This can be achieved in two ways. At HERA, all magnets are fed by one power supply. This results in good tracking of bending power and focal strength. In total 10 mechanical switches break the circuit in case of a quench into nine pieces separated by resistors, in fact, just steel pipes. The resistors are matched to the inductance such that the centres of the resistors and of the nine magnet strings are virtually at ground potential. Hence the ring virtually breaks up into nine independent sub-circuits. If a switch fails to open, the symmetry is broken; therefore the installation of an additional equalising line is necessary. The solution for RHIC, shown in Fig. 18, is similar. One twin power supply feeds one of the two rings. The subdivision follows of course the geometry of the tunnel and the switches consist of thyristors.

Very large rings contain so much energy that the virtual subdivision is not safe enough. Figure 19 shows one of the proposed solutions for the LHC [31]. The accelerator is divided into 16 independent units each of which stores more than HERA. An equal number of circuit breakers and dump resistors are required. The fact that each half octant can be switched off independently is clearly an advantage. A further division is unfortunately excluded from the geography of the LEP tunnel. On the contrary, cost optimisation may lead to a solution employing only one power supply per octant.

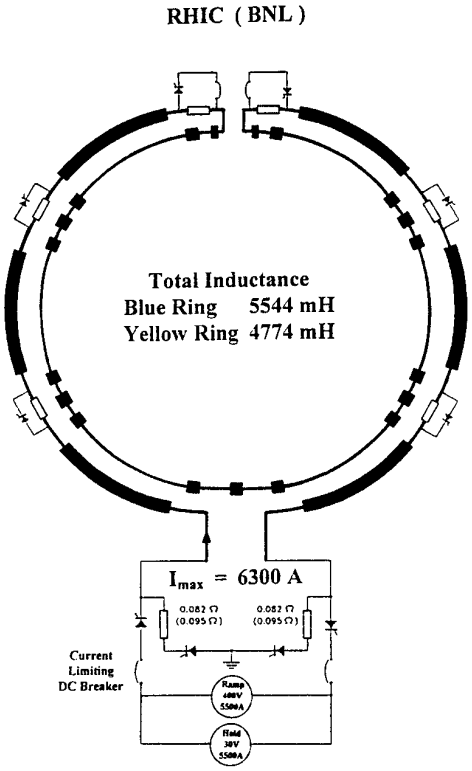

Fig. 18 The proposed connection scheme for one of the RHIC magnet rings. The second ring is almost identically to the one shown.

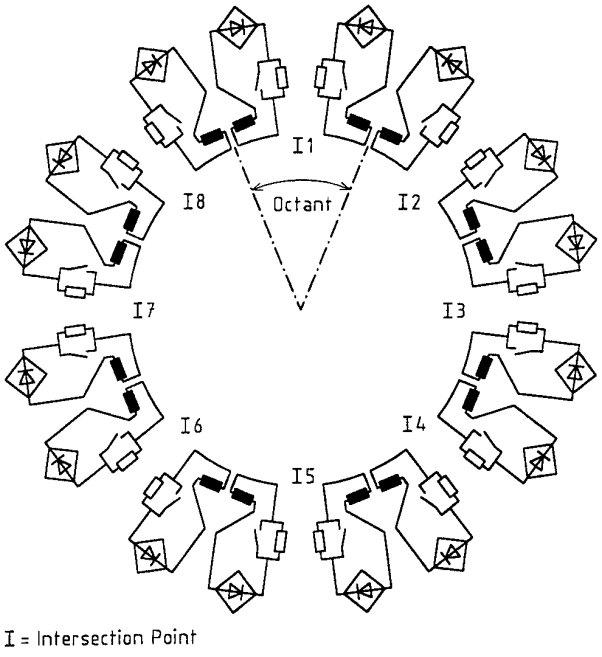

Fig. 19 The proposed subdivision of the LHC magnet string. The number of power supplies may be changed.

7. SUMMARY

Effective quench protection cannot be added afterwards. It is an integral part of the magnet and system design from the very beginning. The costs for cumbersome and complicated protection should be weighed against the cost of more stabilisation copper.

Moreover aspects of reliability play also an important role. Quenches can and will always happen. Hence the quench protection has to be reliable and fail safe. Heaters should be added if necessary, and the overall layout of the power circuit has to be planned and simulated carefully. Magnetic coupling can add to the problems but it can also be turned into an advantage by spreading quenches over large volumes. A low energy density in a quenching magnet has to be tolerated and quench protection is basically the combination of measures to keep the energy density low in case of a quench.

* * *

REFERENCES

[1] M.S. Lubell, IEEE Trans. Magn., Vol 19, 1983, p754ff

[2] M. Wilson, Superconducting Magnets, Oxford Science Publication, Clarendon Press, Oxford

[3] A. Devred, Quench Origins, The physics of particle accelerators, Vol 2, M. Month et al (ed), 1992, American Institute of Physics

[4] H. Maeda et al, Cryogenics, June 1982, p287ff

[5] S. Wipf, Stability and Degradation of Superconducting Current Carrying Devices, Los Alamos 7275, 1978

[6] Maddock et al., Cryogenics 9 (1969), p261ff

[7] K.-Y. Ng, Minimum Propagating Zone of the SSC Superconducting Dipole Cable, SSC-180, 1988

[8] D. Bonmann et al, Investigations on Heater Induced Quenches in a Superconducting Test Dipole Coil for the HERA Proton Accelerator, DESY-HERA 87-13 (1987)

[9] H. Nomuraet al, Cryogenics, 1980, p283ff

[10] J. Chikaba et al, Cryogenics 1990, Vol 30, p649ff

[11] D. Leroy et al, IEEE Trans. Appl Sup Vol 3, pp 781ff,1993

[12] A. Siemko et al, Quench Localization in the Superconducting Model Magnets for the LHC by means of Pick-up Coils, to be published in IEEE Trans. Mag.

[13] T. Ogitsu et al, IEEE Trans. Mag Vol 30, No 4, p2773ff, 1993

[14] T. Ogitsu, Influence of Cable Eddy Currents on the Magnetic Field of Superconducting Particle Accelerator Magnets, SSCL-N-848, 1994 and Thesis (Institute of Applied Physics, University Tsukuba, Japan, 1994)

[15] W.H. Cherry, G.I. Gittelman, Solid State Electronics 1 [1960], p287ff

[16] Buznikov et al, Cryogenics, Vol 34, 1994, p761ff

[17] M.N. Wilson, Computer Simulation of the Quenching of a Superconducting Magnet, Rutherford High Energy Laboratory, RHEL/M 151, 1968

[18] K. Koepke, TMAX program, Fermilab, Batavia, Illinois, USA

[19] U. Otterpohl, Untersuchungen zum Quenchverhalten supraleitender Magnete, DESY-HERA 84/05 and Diploma Thesis, University Hamburg

[20] T. Tominaka et al., IEEE Trans. Mag Vol 28, 1992, p727ff

[21] Pissanetzky et al., Full Featured Implementation of Quench Simulation in Superconducting Magnets, Cryogenics, Vol 34,

[22] D. Hagedorn et al, Modelling of the Quenching Process in Complex Superconducting Magnet Systems, 12th International Conference on Magnet Technology, Leningrad 1991, LHC Note 159

[23] L. Bottura et al, Cryogenics, Vol 32, 1992, p 659ff

[24] L. Bottura et al, Cryogenics, Vol 32, 1992, p 719ff

[25] M.A. Hilal et al., IEEE Trans. Appl. Superconductivity, Vol 4, N03, 1994, p109ff

[26] P.F. Smith, The Review of Scientific Instr., 1963, Vol 34, p368ff

[27] I.M. Bolotin et al, The Quench Detector on Magnetic Modulator or the UNK Quench Protection System, Supercollider 4, J. Nonte ed., Plenum Press, NY, 1992

[28] J.G. Cottingham, Magnet Fault Protection, BNL-16816 (1971)

[29] D. Hagedorn, W. Nägele, Quench Protection Diodes for the Large Hadron Collider LHC at CERN, 1991 Cryogenic Engineering Conference, Huntsville, Alabama, LHC Note 148

[30] G. Ganetis, A. Stevens, Results of Quench Protection Experiment on DM1-031, SSC technical Note No 12, Brookhaven National Laboratory

[31] L. Coull et al, LHC Magnet Quench Protection System, 13th Intern. Conference on Magnet Technology (MT13), Victoria, Canada, 1993, LHC Note 251

BIBLIOGRAPHY

M. Wilson, Superconducting Magnets, Oxford Science Publication, Clarendon Press, Oxford.